

Updated version including supplementary material of the article published  
([http://www.worldscientific.com/doi/pdf/10.1142/9789814329033\\_0002](http://www.worldscientific.com/doi/pdf/10.1142/9789814329033_0002)  
[www.worldscientific.com/doi/suppl/10.1142/8014/suppl\\_file/8014\\_errata.pdf](http://www.worldscientific.com/doi/suppl/10.1142/8014/suppl_file/8014_errata.pdf))

by World Scientific (Singapore) in the Proceedings of the  
12th ICATPP Conference

Villa Olmo (Como, Italy), 7–8 October, 2010.

## Nuclear and Non-Ionizing Energy-Loss for Coulomb Scattered Particles from Low Energy up to Relativistic Regime in Space Radiation Environment

M.J. Boschini<sup>1,2</sup>, C. Consolandi<sup>\*,1</sup>, M. Gervasi<sup>1,3</sup>, S. Giani<sup>4</sup>,  
D. Grandi<sup>1</sup>, V. Ivanchenko<sup>4</sup>, S. Pensotti<sup>3</sup>, P.G. Rancoita<sup>\*\*,1</sup>, M. Tacconi<sup>1</sup>

<sup>1</sup>*INFN-Milano Bicocca, P.zza Scienza, 3 Milano, Italy*

<sup>2</sup>*CILEA Via R. Sanzio, 4 Segrate, MI-Italy*

<sup>3</sup>*Milano Bicocca University, Piazza della Scienza, 3 Milano, Italy*

<sup>4</sup>*CERN, Geneva, 23, CH-1211, Switzerland*

*\* E-mail: [cristina.consolandi@mib.infn.it](mailto:cristina.consolandi@mib.infn.it)*

*\*\* E-mail: [piergiorgio.rancoita@mib.infn.it](mailto:piergiorgio.rancoita@mib.infn.it)*

In the space environment, instruments onboard of spacecrafts can be affected by displacement damage due to radiation. The differential scattering cross section for screened nucleus–nucleus interactions - i.e., including the effects due to screened Coulomb nuclear fields -, nuclear stopping powers and non-ionization energy losses are treated from about 50 keV/nucleon up to relativistic energies.

### 1. Introduction

In the space environment near Earth, low energy particles are, for instance, found trapped within the radiation belts and are partially coming from the Sun. On the other hand, the energies of Galactic Cosmic Rays (GCR) extend up to relativistic range. Protons are the most abundant, but alpha particles and heavier nuclei are also present (e.g., see Sections 4.1.2–4.1.2.5 of Ref. [1]). Abundances and energy spectra of GCRs depend on the position inside the solar cavity and are affected by the solar activity. Above (30–50) MeV/nucleon, the dominant radiation consists of GCRs. At lower energies, from 1 MeV/nucleon up to about 30 MeV/nucleon, one also finds the so-called Anomalous Cosmic Rays (ACRs). GCRs can reach Earth’s magnetosphere and interact with upper layers of the atmosphere. These interactions produce secondary particles, like for example protons with (10–100) MeV energies, which may - in turn - become trapped within the ra-

diation belts. In addition, during transient phenomena like solar flares and coronal mass ejections, Solar Energetic Particles (SEP) are produced in the energy range from few keV's to GeV's.

All these energetic particles can inflict permanent damages to onboard electronic devices employed in space missions. While passing through matter, they can lose energy by Coulomb interactions with electrons (*electronic energy-loss*) and nuclei (*nuclear energy-loss*) of the material. In particular, the nuclear energy-loss - due to screened Coulomb scattering on nuclei of the medium - is relevant for the creation of permanent defects inside the lattice of the material; thus, for instance, it is mostly responsible for the displacement damage which is a cause of degradation of silicon devices.

The developed model - presented in this article - for screened Coulomb elastic scattering up to relativistic energies is included into Geant4 distribution [2] and is available with Geant4 version 9.4 (December 2010).

## 2. Nucleus–Nucleus Interactions and Screened Coulomb Potentials

At small distances from the nucleus, the potential energy is a Coulomb potential, while - at distances larger than the Bohr radius - the nuclear field is screened by the fields of atomic electrons. The interaction between two nuclei is usually described in terms of an interatomic Coulomb potential (e.g., see Section 2.1.4.1 of Ref. [1] and Section 4.1 of Ref. [3]), which is a function of the radial distance  $r$  between the two nuclei

$$V(r) = \frac{zZe^2}{r} \Psi_{\text{I}}(r_{\text{r}}), \quad (1)$$

where  $ez$  (projectile) and  $eZ$  (target) are the charges of the bare nuclei and  $\Psi_{\text{I}}$  is the *interatomic screening function*. This latter function depends on the *reduced radius*  $r_{\text{r}}$  given by

$$r_{\text{r}} = \frac{r}{a_{\text{I}}}, \quad (2)$$

where  $a_{\text{I}}$  is the so-called *screening length* (also termed *screening radius*). In the framework of the Thomas–Fermi model of the atom (e.g., see Chapters 1 and 2 of Ref. [4]) - thus, following the approach of ICRU Report 49 (1993) -, a commonly used screening length for  $z = 1$  incoming particles is that from Thomas–Fermi (e.g., see Refs. [5, 6])

$$a_{\text{TF}} = \frac{C_{\text{TF}} a_0}{Z^{1/3}}, \quad (3)$$

and - for incoming particles with  $z \geq 2$  - that introduced by Ziegler, Biersack and Littmark (1985) (and termed *universal screening length*<sup>a</sup>)

$$a_U = \frac{C_{TF} a_0}{z^{0.23} + Z^{0.23}}, \quad (4)$$

where

$$a_0 = \frac{\hbar^2}{me^2}$$

is the Bohr radius,  $m$  is the electron rest mass and

$$C_{TF} = \frac{1}{2} \left( \frac{3\pi}{4} \right)^{2/3} \simeq 0.88534$$

is a constant introduced in the Thomas–Fermi model.

The simple scattering model due to Wentzel [10] - with a single exponential screening-function  $\Psi_I(r_r)$  {e.g., see Ref. [10] and Equation (21) in Ref. [11]} - was repeatedly employed in treating single and multiple Coulomb-scattering with screened potentials (e.g., see Ref. [11] - and references therein - for a survey of such a topic and also Refs. [12–15]). The resulting elastic differential cross section differs from the Rutherford differential cross section by an additional term - the so-called *screening parameter* - which prevents the divergence of the cross section when the angle  $\theta$  of scattered particles approaches  $0^\circ$ . The screening parameter  $A_{s,M}$  [e.g., see Equation (21) of Bethe (1953)] - as derived by Molière (1947, 1948) for the single Coulomb scattering using a Thomas–Fermi potential - is expressed<sup>b</sup> as

$$A_{s,M} = \left( \frac{\hbar}{2p a_I} \right)^2 \left[ 1.13 + 3.76 \times \left( \frac{\alpha z Z}{\beta} \right)^2 \right] \quad (5)$$

where  $a_I$  is the screening length - from Eqs. (3, 4) for particles with  $z = 1$  and  $z \geq 2$ , respectively;  $\alpha$  is the fine-structure constant;  $p$  ( $\beta c$ ) is the momentum (velocity) of the incoming particle undergoing the scattering onto a target supposed to be initially at rest;  $c$  and  $\hbar$  are the speed of light and the reduced Planck constant, respectively. When the (relativistic) mass

<sup>a</sup>Another screening length commonly used is that from Lindhard and Sharff (1961) (e.g., see Ref. [8] ; see also Ref. [9] and references therein):

$$a_L = \frac{C_{TF} a_0}{(z^{2/3} + Z^{2/3})^{1/2}}.$$

<sup>b</sup>It has to be remarked that the screening radius originally used in Refs. [12, 13] was that from Eq. (3).

- with corresponding rest mass  $m$  - of the incoming particle is much lower than the rest mass ( $M$ ) of the target nucleus, the differential cross section - obtained from the Wentzel–Molière treatment of the single scattering - is:

$$\frac{d\sigma^{\text{WM}}(\theta)}{d\Omega} = \left(\frac{zZe^2}{p\beta c}\right)^2 \frac{1}{(2A_{s,M} + 1 - \cos\theta)^2} \quad (6)$$

$$= \left(\frac{zZe^2}{2p\beta c}\right)^2 \frac{1}{[A_{s,M} + \sin^2(\theta/2)]^2} \quad (7)$$

(e.g., see Section 2.3 in Ref. [11] and references therein). Equation (7) differs from Rutherford’s formula - as already mentioned - for the additional term  $A_{s,M}$  to  $\sin^2(\theta/2)$ . The corresponding total cross section {e.g., see Equation (25) in Ref. [11]} per nucleus is

$$\sigma^{\text{WM}} = \left(\frac{zZe^2}{p\beta c}\right)^2 \frac{\pi}{A_{s,M}(1 + A_{s,M})}. \quad (8)$$

Thus, for  $\beta \simeq 1$  (i.e., at very large  $p$ ) and with  $A_{s,M} \ll 1$ , from Eqs. (5, 8) one finds that the cross section approaches a constant:

$$\sigma_c^{\text{WM}} \simeq \left(\frac{2zZe^2 a_I}{\hbar c}\right)^2 \frac{\pi}{1.13 + 3.76 \times (\alpha z Z)^2}. \quad (9)$$

In case of a scattering under the action of a central potential (for instance that due to a screened Coulomb field), when the rest mass of the target particle is no longer much larger than the relativistic mass of the incoming particle, the expression of the differential cross section must properly be re-written - in the center of mass system - in terms of an “effective particle” with momentum ( $p'_r$ ) equal to that of the incoming particle ( $p'_{in}$ ) and rest mass equal to the relativistic reduced mass

$$\mu_{\text{rel}} = \frac{mM}{M_{1,2}},$$

where  $M_{1,2}$  is the invariant mass;  $m$  and  $M$  are the rest masses of the incoming and target particles, respectively (e.g., see Refs. [15–17] and references therein). The “effective particle” velocity is given by:

$$\beta_r c = c \sqrt{\left[1 + \left(\frac{\mu_{\text{rel}} c}{p'_{in}}\right)^2\right]^{-1}}.$$

Thus, the differential cross section<sup>f</sup> per unit solid angle of the incoming particle results to be given by

$$\frac{d\sigma^{\text{WM}}(\theta')}{d\Omega'} = \left( \frac{zZe^2}{2p'_{in}\beta_r c} \right)^2 \frac{1}{[A_s + \sin^2(\theta'/2)]^2}, \quad (10)$$

with

$$A_s = \left( \frac{\hbar}{2p'_{in} a_1} \right)^2 \left[ 1.13 + 3.76 \times \left( \frac{\alpha z Z}{\beta_r} \right)^2 \right] \quad (11)$$

and  $\theta'$  the scattering angle in the center of mass system.

The energy<sup>c</sup>  $T$  transferred to the recoil target is related to the scattering angle as  $T = T_{max} \sin^2(\theta'/2)$  - where  $T_{max}$  is the maximum energy which can be transferred in the scattering (e.g., see Section 1.5 of Ref. [1]) -, thus, assuming an isotropic azimuthal distribution one can re-write Eq. (10) in terms of the kinetic energy transferred from the projectile -, i.e.,  $[-T]$ , where the negative sign indicates that energy is lost by the projectile - to the recoil target as

$$\begin{aligned} d\sigma^{\text{WM}} &= \left( \frac{zZe^2}{2p'_{in}\beta_r c} \right)^2 \frac{1}{[A_s + \sin^2(\theta'/2)]^2} \sin(\theta') d\theta' \int_0^{2\pi} d\phi \\ &= \pi \left( \frac{zZe^2}{p'_{in}\beta_r c} \right)^2 \frac{T_{max}}{[T_{max} A_s + T]^2} d[-T]. \end{aligned} \quad (12)$$

Finally, from Eq. (12), the differential cross section with respect to the kinetic recoil energy ( $T$ ) of the target is given by:

$$\frac{d\sigma^{\text{WM}}(T)}{dT} = \pi \left( \frac{zZe^2}{p'_{in}\beta_r c} \right)^2 \frac{T_{max}}{[T_{max} A_s + T]^2}. \quad (13)$$

<sup>f</sup>By inspection of Eqs. (5, 7, 10, 11), one finds that for  $\beta_r \cong 1$  the cross section is given by Eq. (9).

<sup>c</sup>One can show - e.g., see Section 1.5 of Ref. [1] - that the four momentum transfer is given by

$$t = -2MT.$$

Since  $t$  is invariant, then the kinetic energy transferred is also invariant. Furthermore, since  $T = T_{max} \sin^2(\theta'/2)$ , then one finds that

$$d[-T] = T_{max} d[-\sin^2(\theta'/2)] = \frac{T_{max}}{2} \sin(\theta') d\theta'$$

(e.g., see Section 1.5 of Ref. [1]).

Furthermore, since

$$\begin{aligned}\beta_{rc} &= \frac{pc^2}{E} \\ p'_{in} &= \frac{pM}{M_{1,2}} \\ T_{max} &= \frac{2p^2M}{M_{1,2}^2}\end{aligned}\quad (14)$$

with  $p$  and  $E$  the momentum and total energy of the incoming particle in the laboratory, then one finds

$$\frac{T_{max}}{(p'_{in} \beta_{rc})^2} = \frac{2E^2}{p^2Mc^4}.$$

Therefore, Eq. (13) can be re-written as

$$\frac{d\sigma^{WM}(T)}{dT} = 2\pi (zZe^2)^2 \frac{E^2}{p^2Mc^4} \frac{1}{[T_{max} A_s + T]^2}. \quad (15)$$

Equation (15) expresses - as already mentioned - the differential cross section as a function of the (kinetic) energy  $T$  achieved by the recoil target.

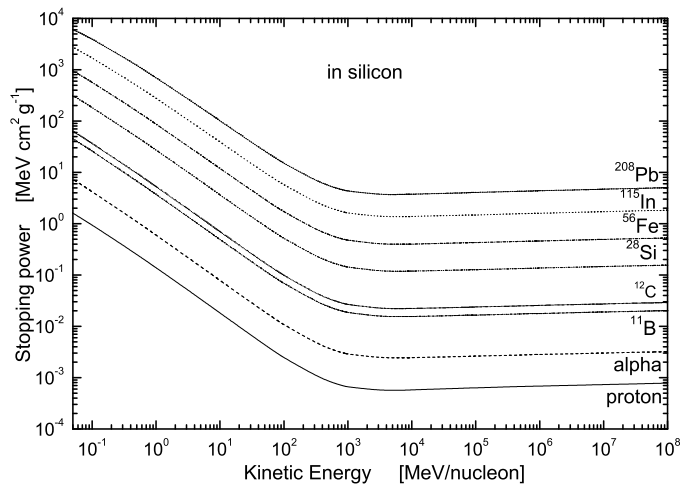


Fig. 1. Nuclear stopping power - in  $\text{MeV cm}^2 \text{g}^{-1}$  - calculated using Eq. (17) in silicon is shown as a function of the kinetic energy per nucleon - from 50 keV/nucleon up to 100 TeV/nucleon - for protons,  $\alpha$ -particle and  $^{11}\text{B}$ ,  $^{12}\text{C}$ ,  $^{28}\text{Si}$ ,  $^{56}\text{Fe}$ ,  $^{115}\text{In}$ ,  $^{208}\text{Pb}$ -nuclei.

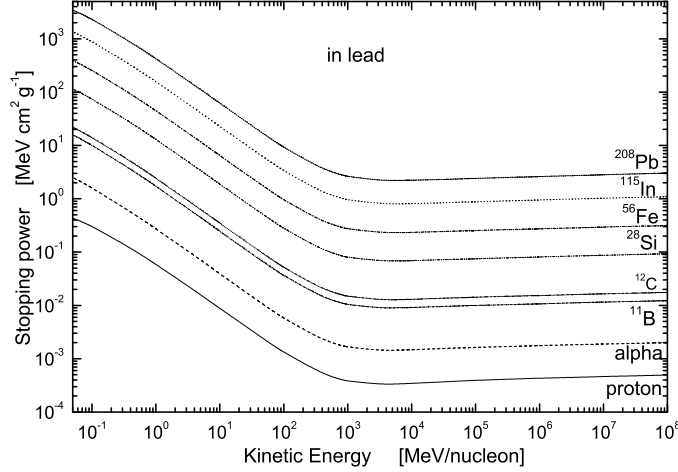


Fig. 2. Nuclear stopping power - in  $\text{MeV cm}^2 \text{g}^{-1}$  - calculated using Eq. (17) in lead is shown as a function of the kinetic energy per nucleon - from 50 keV/nucleon up 100 TeV/nucleon - for protons,  $\alpha$ -particles and  $^{11}\text{B}$ -,  $^{12}\text{C}$ -,  $^{28}\text{Si}$ -,  $^{56}\text{Fe}$ -,  $^{115}\text{In}$ -,  $^{208}\text{Pb}$ -nuclei.

### 3. Nuclear Stopping Power

Using Eq. (15) the nuclear stopping power - in  $\text{MeV cm}^{-1}$  - is obtained as

$$\begin{aligned}
 -\left(\frac{dE}{dx}\right)_{\text{nucl}} &= n_A \int_0^{T_{max}} \frac{d\sigma^{\text{WM}}(T)}{dT} T dT & (16) \\
 &= 2 n_A \pi (zZe^2)^2 \frac{E^2}{p^2 M c^4} \int_0^{T_{max}} \frac{T}{[A_s T_{max} + T]^2} dT \\
 &= 2 n_A \pi (zZe^2)^2 \frac{E^2}{p^2 M c^4} \left[ \frac{A_s}{A_s + 1} - 1 + \ln \left( \frac{A_s + 1}{A_s} \right) \right] & (17)
 \end{aligned}$$

with  $n_A$  the number of nuclei (atoms) per unit of volume and, finally, the negative sign indicates that the energy is lost by the incoming particle (thus, achieved by recoil targets). For energies higher than a few tens of keVs, because  $A_s \ll 1$ , Eq. (17) can be re-written as

$$-\left(\frac{dE}{dx}\right)_{\text{nucl}} = 2 \pi n_A (zZe^2)^2 \frac{E^2}{p^2 M c^4} \left[ \ln \left( \frac{1}{A_s} \right) - 1 \right]. \quad (18)$$

It has to be noted that, as the incoming momentum increases to a value for which  $p \simeq E$ , the set of terms - in front of those included in brackets - decreases and approaches a constant; while the term  $\ln(1/A_s)$  increases as  $\ln(p)$  for  $E \gg mc^2, Mc^2$  [e.g., see Eqs. (11, 14)]. Thus, a slight increase of the nuclear stopping power with energy is expected because of the decrease of the screening parameter with energy.

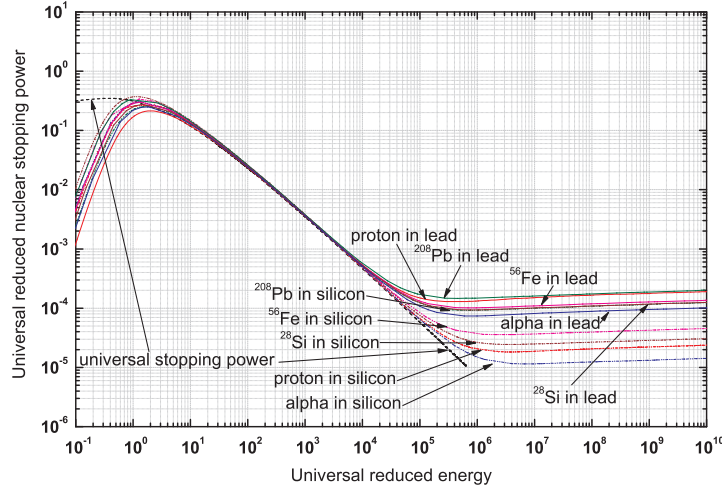


Fig. 3. Universal stopping power (dashed line) as a function of the universal reduced energy [Eq. (19)]. The other curves correspond to the dimensionless nuclear stopping power obtained from Eq. (17) - for protons,  $\alpha$ -particles,  $^{28}\text{Si}$ -,  $^{56}\text{Fe}$ -,  $^{208}\text{Pb}$ -nuclei in silicon (Fig. 1) and lead (Fig. 2) absorbers - and divided by the parameter  $\mathbb{K}$  [Eq. (21)].

For instance, in Fig. 1 (Fig. 2) the nuclear stopping power in silicon (in lead) - in  $\text{MeV cm}^2 \text{g}^{-1}$  - is shown as a function of the kinetic energy per nucleon - from 50 keV/nucleon up 100 TeV/nucleon - for protons,  $\alpha$ -particles and  $^{11}\text{B}$ -,  $^{12}\text{C}$ -,  $^{28}\text{Si}$ -,  $^{56}\text{Fe}$ -,  $^{115}\text{In}$ -,  $^{208}\text{Pb}$ -nuclei.

It has to be remarked that - at very low energies - the Wentzel-Molière nuclear stopping power [Eq. (17)] differs from that obtained by Ziegler, Biersack and Littmark (1985) using the so-called *universal screening potential* (see also Ref. [18]). However, they have shown (e.g., see Figure 2-18 in Ref. [7] or, equivalently, Figure 2-18 in Ref. [18]) that different screening potentials - including the Bohr potential in which  $\Psi_{\text{I}}(r_{\text{r}})$  is assumed to be an exponential function similarly to Wentzel's assumption - result in nuclear stopping powers which exhibit marginal differences for  $\epsilon_{\text{r,U}}$  above 10 (see also Fig. 3).  $\epsilon_{\text{r,U}}$  is the so-called *universal reduced energy* expressed as:

$$\epsilon_{\text{r,U}} = \frac{\mathbb{R}}{zZ(z^{0.23} + Z^{0.23})} \left( \frac{M}{m + M} \right) E_k, \quad (19)$$

where  $E_k$  is in MeV and the numerical constant is  $\mathbb{R} = 32.536 \times 10^3 \text{ MeV}^{-1}$  {e.g., see Equation (2-73) of Ref. [7] or Equation (2-88) of Ref. [18], see also Section 2.1.4.1 of Ref. [1]}. For instance, in silicon  $\epsilon_{\text{r,U}} \simeq 10$  corresponds to  $E_k \simeq 13 \text{ keV}$  [67 keV/nucleon] for protons [lead nuclei]. Ziegler, Biersack and Littmark (1985) provided a general expression for the nuclear stopping



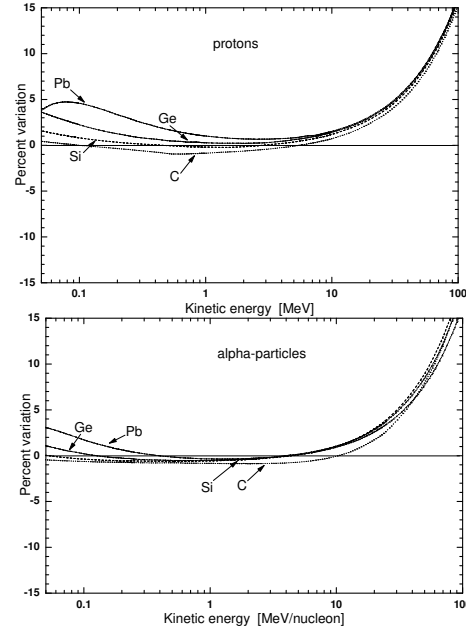


Fig. 4. Variation (in percentage) of nuclear stopping powers - calculated with Eq. (17) for energies from 50 keV/nucleon up to 100 MeV/nucleon - with respect to ICRU tabulated values [3] as a function of the kinetic energy in MeV/nucleon, for protons (top) and  $\alpha$ -particles (bottom) traversing amorphous carbon, silicon, germanium and lead media.

power (e.g., see Section 2.1.4.1 of Ref. [1]), i.e.,

$$-\left(\frac{dE}{dx}\right)_{\text{nucl}}^{\text{U}} = \mathbb{K} \mathfrak{R}(\epsilon_{r,\text{U}}) \text{ [MeV/cm]}, \quad (20)$$

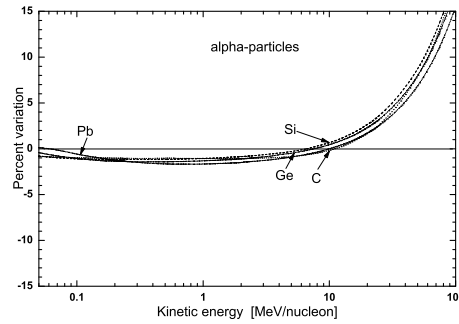


Fig. 5. Variation (in percentage) of nuclear stopping powers - calculated with Eq. (17) with the expressions (22, 23) for the screening parameter - with respect to ICRU tabulated values [3] as a function of the kinetic energy in MeV/nucleon, for  $\alpha$ -particles traversing amorphous carbon, silicon, germanium and lead media for energies from 50 keV/nucleon up to 100 MeV/nucleon.

18

with

$$\mathbb{K} \simeq 5.1053 \times 10^3 \frac{\rho z Z}{A(1 + M/m)(z^{0.23} + Z^{0.23})} \text{ [MeV/cm]} \quad (21)$$

where  $\rho$  and  $A$  are the density and atomic weight of the target medium, respectively;  $\mathfrak{R}(\epsilon_{r,U})$  - the so-called (*universal*) *reduced nuclear stopping power* [termed, also, (*universal*) *scaled nuclear stopping power*] given in Equations (2-89)–(2-90) in Ref. [18] (see also page 80 in Ref. [1]) - is dimensionless. Additionally, the present calculations can be compared with values of stopping powers - obtained using the universal screened potential - available in SRIM (2008) [19]. Usually an agreement - to better than a few percents - is achieved down to about 150 keV/nucleon, where - for instance - one finds  $\approx 5.5$  (9.9) % for  $\alpha$ -particles (lead ions) in silicon. At large energies, the non-relativistic approach due to Ziegler, Biersack and Littmark (1985) becomes less appropriate and deviations from stopping powers calculated by means of the universal screening potential are expected and observed for  $\epsilon_{r,U} \gtrsim (1.5\text{--}2.5) \times 10^4$  (e.g., see Fig. 3).

The non-relativistic approach - based on the universal screening potential - of Ziegler, Biersack and Littmark (1985) was also used by ICRU (1993) to calculate nuclear stopping powers - currently available on the web (e.g., see Ref. [20]) - due to protons and  $\alpha$ -particles in materials. ICRU (1993) used as screening lengths those from Eqs. (3, 4) for protons and  $\alpha$ -particles, respectively. In Fig. 4, the variation (in percentage) of nuclear stopping powers - calculated with Eq. (17) - with respect to ICRU tabulated values [3] is shown as a function of the kinetic energy per nucleon (in MeV/nucleon) - for energies from 50 keV/nucleon up to 100 MeV/nucleon - for protons and  $\alpha$ -particles traversing amorphous carbon, silicon, germanium and lead media. The stopping powers for protons ( $\alpha$ -particles) from Eq. (17) are less than  $\approx 5\%$  larger than those reported by ICRU (1993) from 50 keV/nucleon up to  $\approx 32$  MeV (31 MeV/nucleon) - the upper energy corresponds to  $\epsilon_{r,U} \approx 6.2 \times 10^4$  ( $4.3 \times 10^4$ ) for protons in an amorphous carbon ( $\alpha$ -particles in a silicon) medium -. At larger energies the stopping powers from Eq. (17) largely differ from those from ICRU - as expected - due to the complete relativistic treatment of the present approach.

The simple screening parameter used so far [Eq. (11)] - derived by Molière (1947) - can be modified by means of a *practical correction*, i.e.,

$$A'_s = \left( \frac{\hbar}{2 p'_{in} a_I} \right)^2 \left[ 1.13 + 3.76 \times \mathbb{C} \left( \frac{\alpha z Z}{\beta_r} \right)^2 \right], \quad (22)$$

to achieve a better agreement with low energy calculations of Ziegler, Bier-sack and Littmark (1985). For instance, for protons,  $\alpha$ -particles and heavier ions, with

$$C = (10\pi z Z \alpha)^{0.04} \quad (23)$$

the stopping powers obtained from Eq. (17) - in which  $A'_s$  replaces  $A_s$  - differ from the values of SRIM (2008) by less than  $\approx 3.5$  (2.6) % for  $\alpha$ -particles (lead ions) in silicon down to about 50 keV/nucleon. With respect to the tabulated values of ICRU (1993), the agreement for  $\alpha$ -particles is usually better than 2% at low energy down to 50 keV/nucleon (Fig. 5) - a 1% agreement is achieved at about 50 keV/nucleon in case of a carbon (or silicon) medium. At very high energy, the stopping power is slightly affected when  $A'_s$  replaces  $A_s$ : for example, a) in silicon at 100 TeV/nucleon the nuclear stopping power of  $\alpha$ -particles (lead-ions) is decreased by about 0.03 (0.71) % and b) in lead it is decreased by about 0.4 (1.0) %. It has to be remarked that a more appropriate expression for the screening parameter and a practical correction factor may require a further understanding.

#### 4. Non-Ionizing Energy Loss due to Coulomb Scattering

A relevant process - which causes permanent damage to the silicon bulk structure - is the so-called *displacement damage* (e.g., see Chapter 4 of Ref. [1], Refs. [21–23] and references therein). Displacement damage may be inflicted when a *primary knocked-on atom* (PKA) is generated. The interstitial atom and relative vacancy are termed Frenkel-pair (FP). In turn, the displaced atom may have sufficient energy to migrate inside the lattice and - by further collisions - can displace other atoms as in a collision cascade. This displacement process modifies the bulk characteristics of the device and causes its degradation. The total number of FPs can be estimated calculating the energy density deposited from displacement processes. In turn, this energy density is related to the *Non-Ionizing Energy Loss* (NIEL), i.e., the energy per unit path lost by the incident particle due to displacement processes.

In case of Coulomb scattering on nuclei, the non-ionizing energy-loss can be calculated using the Wentzel–Molière differential cross section [Eq. (15)] discussed in Sect. 2, i.e.,

$$-\left(\frac{dE}{dx}\right)_{\text{nucl}}^{\text{NIEL}} = n_A \int_{T_d}^{T_{max}} T L(T) \frac{d\sigma^{\text{WM}}(T)}{dT} dT, \quad (24)$$

where  $E$  is the kinetic energy of the incoming particle,  $T$  is the kinetic energy transferred to the target atom,  $L(T)$  is the fraction of  $T$  deposited

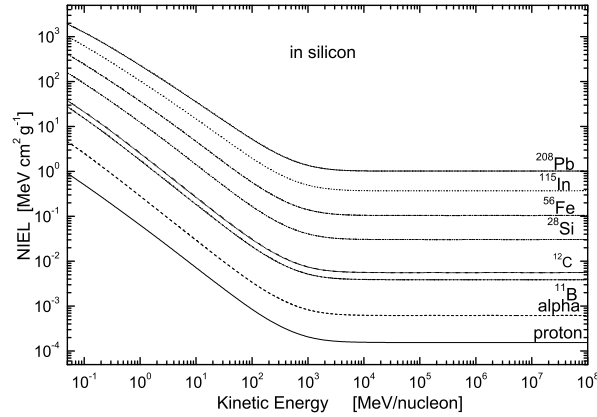


Fig. 6. Non-ionizing stopping power - in  $\text{MeV cm}^2 \text{g}^{-1}$  - calculated using Eq. (24) in silicon is shown as a function of the kinetic energy per nucleon - from 50 keV/nucleon up to 100 TeV/nucleon - for protons,  $\alpha$ -particles and  $^{11}\text{B}$ -,  $^{12}\text{C}$ -,  $^{28}\text{Si}$ -,  $^{56}\text{Fe}$ -,  $^{115}\text{In}$ -,  $^{208}\text{Pb}$ -nuclei. The threshold energy for displacement is 21 eV in silicon.

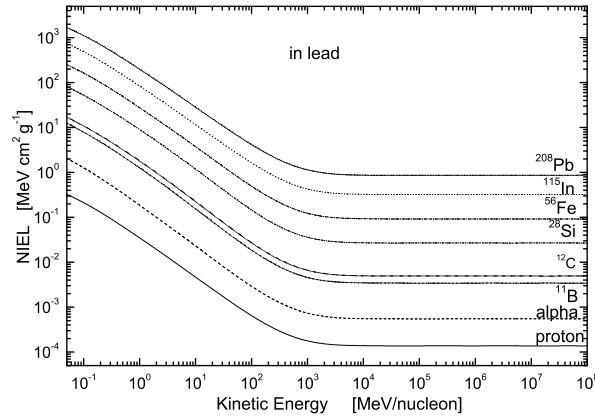


Fig. 7. Non-ionizing stopping power - in  $\text{MeV cm}^2 \text{g}^{-1}$  - calculated using Eq. (24) in lead is shown as a function of the kinetic energy per nucleon - from 50 keV/nucleon up to 100 TeV/nucleon - for protons,  $\alpha$ -particles and  $^{11}\text{B}$ -,  $^{12}\text{C}$ -,  $^{28}\text{Si}$ -,  $^{56}\text{Fe}$ -,  $^{115}\text{In}$ -,  $^{208}\text{Pb}$ -nuclei. The threshold energy for displacement is 25 eV in lead

by means of displacement processes. The expression of  $L(T)$  - the so-called *Lindhard partition function* - can be found, for instance, in Refs. [24, 25] and in Equations (4.94, 4.96) of Section 4.2.1.1 in Ref. [1] (see also references therein).  $T_{\text{de}} = T L(T)$  is the so-called *damage energy*, i.e., the energy deposited by a recoil nucleus with kinetic energy  $T$  via displacement damages inside the medium. The integral in Eq. (24) is computed from the minimum energy  $T_d$  - the so-called *threshold energy for displacement*, i.e., that energy necessary to displace the atom from its lattice position - up to

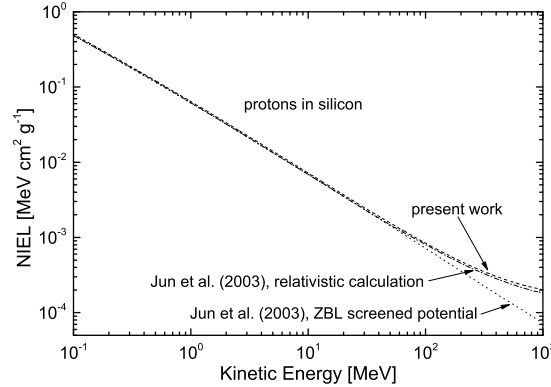


Fig. 8. Non-ionizing stopping powers of protons in silicon with energies from 100 keV up to 1 GeV: data for the dashed-dotted and dotted lines are the relativistic and Ziegler-Biersack-Littmark screened potential calculations from Jun and collaborators (2003), respectively (e.g., see Ref. [26]); data for the dashed line are obtained from Eq. (24) (e.g., see Fig. 6).

the maximum energy  $T_{max}$  that can be transferred during a single collision process.  $T_d$  is about 21 eV in silicon (e.g., see Table 1 in Ref. [26] and references therein) and 25 eV in lead (e.g., see Table 22 at page 83 in Ref. [27] and references therein). For instance, in Fig. 6 (Fig. 7) the non-ionizing energy loss - in  $\text{MeV cm}^2 \text{g}^{-1}$  - in silicon (lead) is shown as a function of the kinetic energy per nucleon - from 50 keV/nucleon up to 100 TeV/nucleon - for protons,  $\alpha$ -particles and  $^{11}\text{B}$ -,  $^{12}\text{C}$ -,  $^{28}\text{Si}$ -,  $^{56}\text{Fe}$ -,  $^{115}\text{In}$ -,  $^{208}\text{Pb}$ -nuclei. As already remarked by Boschini and collaborators (2010), at high energy the Coulomb NIEL - similarly to the nuclear stopping power - does not decrease with energy as it is found by Ziegler, Biersack and Littmark (1985) or in other calculations based on their universal screening potential derived in the framework of a non-relativistic treatment of the screened Coulomb scattering.

Furthermore, Jun and collaborators (2003) have already demonstrated that a relativistic treatment [24] of Coulomb scattering of protons - with kinetic energies above 50 MeV - upon silicon results into a non-ionizing energy loss which is larger than that expected from calculations using the Ziegler-Biersack-Littmark screened potential with a universal screening length (e.g., see Refs. [7, 25, 26]). The relativistic cross section used for treating the Coulomb scattering is the one derived by McKinley and Feshbach (1948) to describe the scattering of electrons on nuclei (e.g., see Section 4.2.1.4 of Ref. [1] and references therein). Seitz and Koehler (1956) suggested that - when the mass of the projectile is much lower than the target rest-mass (e.g., see Section 13 of Ref. [29] and references therein)

- this cross section can also describe - although screening effects are neglected - the scattering of protons and light nuclei, thus, providing - at high energy - a damage cross section which does not decrease with increasing energy. The data from Jun and collaborators (2003) - for protons with energies from 100 keV up to 1 GeV - are shown in Fig.8: the Ziegler–Biersack–Littmark (1985) screened potential was used to treat the Coulomb scattering of protons with energies lower than 50 MeV. In the same figure, the data obtained using Eq. (24) - e.g., see Fig. 6 - are also shown. There is an agreement to better than  $\approx 6.5\%$  - achieved at  $\approx 1$  GeV - between the results obtained by Jun and collaborators (2003) and the present calculations.

## 5. Conclusions

The treatment of nucleus–nucleus interactions due to relativistic Coulomb scatterings with screened potentials - like the present approach based on Wentzel–Molière scattering - allows one to determine both the total and differential cross sections, thus, to calculate the resulting nuclear and non-ionizing stopping powers. At high energies, the nuclear stopping powers exhibit a very slight logarithmic increase with energy. At low energies - i.e., above  $\approx 50$  keV/nucleon and up to  $\approx 32$  and  $31$  MeV/nucleon, for protons and  $\alpha$ -particles, respectively -, the present results are in agreement to better than  $\approx 5\%$  with ICRU tabulated values of stopping powers obtained using the universal screening potential for the scattering of protons and  $\alpha$ -particles in matter. An agreement to better than to  $(5.5\text{--}9.9)\%$  - for instance, for a silicon medium - is found with SRIM (2008) values down to 150 keV/nucleon. Furthermore, these calculations are also in agreement to better than  $\approx 6.5\%$  with those obtained by Jun and collaborators (2003) for the non-ionizing stopping powers of protons - with energies from 50 MeV up to 1 GeV - in silicon.

Finally, it has to be remarked that - with a simple correction factor applied to the screening factor - an agreement to a few percents can be achieved with SRIM (2008) stopping powers down to about 50 keV/nucleon. However, a more appropriate expression for the screening parameter and a practical correction factor may require a further understanding.

## References

1. C. Leroy and P.G. Rancoita, *Principles of Radiation Interaction in Matter and Detection*, 2nd Edition, World Scientific (Singapore) 2009.

2. S. Agostinelli et al., Geant4 a simulation toolkit, *Nucl. Instr. and Meth. in Phys. Res. A* 506 (2003), 250-303; see also the website: <http://geant4.cern.ch/>
3. ICRU, ICRU Report 49, Stopping Powers and Ranges for Protons and Alpha Particles (1993).
4. I.M. Torrens, *Interatomic Potentials*, Academic Press (New York) 1972.
5. L.H. Thomas, *Proc. Cambridge Phil. Soc.* 23 (1927), 542.
6. E. Fermi, *Z. Phys.* 48 (1928), 73–79.
7. J.F. Ziegler, J.P. Biersack and U. Littmark, *The Stopping Range of Ions in Solids*, Vol. 1, Pergamon Press (New York) 1985.
8. J. Lindhard and M. Sharff, *Phys. Rev.* 124 (1961), 128–130.
9. S. Kalbitzer and H. Oetzmann, *Phys. Lett. A* 59 (1976), 197–198.
10. G. Wentzel, *Z. Phys.* 40 (1926), 590–593.
11. J.M. Fernandez-Vera et al., *Nucl. Instr. and Meth. in Phys. Res. B* 73 (1993), 447–473.
12. von G. Molière, *Z. Naturforsch.* A2 (1947), 133–145; A3 (1948), 78.
13. H. A. Bethe, *Phys. Rev.* 89 (1953), 1256–1266.
14. A. V. Butkevick et al., *Nucl. Instr. and Meth. in Phys. Res. A* 488 (2002), 282-194.
15. M. Boschini et al., *Geant4-based application development for NIEL calculation in the Space Radiation Environment*, Proc. of the 11th ICATPP Conference, October 5–9 2009, Villa Olmo, Como, Italy, World Scientific, Singapore (2010), 698–708, IBSN: 10-981-4307-51-3.
16. A. Staruszewicz and K. Zalewski *Acta Phys. Pol. B* 8 (no. 10) (1977), 815–817.
17. P.P. Fiziev and I.T. Todorov, *Phys. Rev. D* 63 (2001), 104007-1–104007-9.
18. J.F. Ziegler, M.D. Ziegler and J.P. Biersack, *The Stopping and Range of Ions in Matter*, SRIM Co. (Chester.) 2008.
19. SRIM: J.F. Ziegler, M.D. Ziegler and J.P. Biersack, *The Stopping and Range of Ions in Matter*, version 2008.03 (2008), available at: <http://www.srim.org/>
20. M.J. Berger, J.S. Coursey, M.A. Zucker and J. Chang, data from ESTAR, PSTAR and ASTAR (version 1.2.3, August 2005); available on the web site (2010): <http://physics.nist.gov/Star>; originally published as: M.J. Berger, NISTIR 4999, NIST, Gaithersburg, MD (1993).
21. C. Leroy and P.G. Rancoita, *Reports on Progress in Physics* 70, 4 (2007) 493–625.
22. E. Borchi et al., *Nucl. Instr. and Meth. in Phys. Res. A* 279 (1989), 277–280.
23. C. Consolandi et al., *Nucl. Instr. and Meth. in Phys. Res. B* 252 (2006), 276.
24. I. Jun, *IEEE Trans. on Nucl. Sci.* 48 (2001), 162–175
25. S.R. Messenger et al., *IEEE Trans. on Nucl. Sci.* 50 (2003), 1919–1923.
26. I. Jun, M.A Xapsos, S.R. Messenger, E.A. Burke, R.J. Walters, G.P. Summers and T. Jordan, *IEEE Trans. on Nucl. Sci.* 50 (2003), 1924–1928.
27. G.S. Was, *Fundamentals of radiation materials science: metals and alloys* Springer (Berlin), 2007.
28. A.Jr. McKinley and H. Feshbach *Phys. Rev.* 74 (1948), 1759.
29. F. Seitz and J.S. Koehler, *Solid State Physics* vol. 2, edited by F. Seitz and D. Turnbull, Academic Press Inc. (New York), 1956.